Journal of Hazardous Materials 182 (2010) 217–224

Contents lists available at ScienceDirect

Journal of Hazardous Materials

journal homepage: www.elsevier.com/locate/jhazmat

Optimization of preparation of activated carbon from cotton stalk by microwave assisted phosphoric acid-chemical activation

Hui Deng*, Genlin Zhang, Xiaolin Xu, Guanghui Tao, Jiulei Dai

Key Laboratory for Green Processing of Chemical Engineering of Xinjiang Bingtuan, School of Chemistry and Chemical Engineering, Shihezi University, Shihezi 832003, Xinjiang, China

ARTICLE INFO

Article history:
Received 16 November 2009
Received in revised form 3 June 2010
Accepted 4 June 2010
Available online 12 June 2010

Keywords:
Cotton stalk
Orthogonal array experimental design
Microwave radiation
Isotherm
Kinetic

ABSTRACT

The preparation of activated carbon (AC) from cotton stalk was investigated in this paper. Orthogonal array experimental design method was used to optimize the preparation of AC using microwave assisted phosphoric acid. Optimized parameters were radiation power of 400 W, radiation time of 8 min, concentration of phosphoric acid of 50% by volume and impregnation time of 20 h, respectively. The surface characteristics of the AC prepared under optimized condition were examined by pore structure analysis, scanning electron microscopy (SEM) and Fourier transform infrared spectroscopy (FT-IR). Pore structure analysis shows that mecropores constitute more of the porosity of the prepared AC. Compared to cotton stalk, different functionalities and morphology on the carbon surfaces were formed in the prepared process. The adsorption capacity of the AC was also investigated by removing methylene blue (MB) in aqueous solution. The equilibrium data of the adsorption was well fitted to the Langmuir isotherm. The maximum adsorption capacity of MB on the prepared AC is 245.70 mg/g. The adsorption process follows the pseudo-second-order kinetic model.

1. Introduction

Cotton stalk was the largest byproduct in Xinjiang province, in P.R. China, which also stored huge potential energy. It is substantial to make the best use of this potential source. Among all provinces in China, Xinjiang province has the largest cotton-producing area with the best quality of cotton. Data provided from Xinjiang Statistical Center Bureau in 2008 showed that there was an enormous increase in the production of cotton, which was enhanced from 218 to 310 million tones in recent 3 years. The higher production of cotton means the greater output of byproducts. Unfortunately, cotton stalk was disposed by either burning or discarding in Xinjiang.

AC is a carbonaceous material possessing a higher porosity due to which it is commonly used in variety of applications, concerned principally with the removal of chemical species by adsorption from the liquid or gas phase [1]. The high adsorptive capacity of AC is associated with its internal porosity and other properties such as surface area, pore volume and pore size distribution [2]. These properties have been determined not only by the physical properties and the chemical composition of the precursor, but also by the activation process of lignocellulosic precursors [3]. For preparation of AC, conventional heating method is usually adopted, in which the energy is produced by electrical furnace. Similarly, the preparation and characterization of ACs derived from cotton stalk with H_3PO_4 were also usually used by conventional heating method [4–6]. But the problem is that it will still take several hours and incur extra costs for the activation process to reach the desired level of activation in the conventional heating system.

Microwave is now being used in various fields in order to heat dielectric materials because it can considerably shorten treatment time and reduce energy consumption. Conventional heating is surface heating. It generates a thermal gradient from the hot surface of the char particle to its interior which leads to the difficulty of caloric transport. Microwave heating is both internal and volumetric, where the tremendous thermal gradient from the interior of the char particle to its cool surface allows the microwave-induced reaction to proceed more quickly and effectively at a lower bulk temperature, resulting in energy savings and shortening the processing time [7,8]. Recently microwave heating technology has been applied to fabricate AC [8,9].

Orthogonal array design (OAD) is a type of fractional factorial design in which orthogonal array is used to assign factors to a series of experimental combinations [10]. The most significant factors affecting the output can be obtained from both variance (ANOVA) and direct observation analysis [11,12]. Several applications of this method have been reported in various processes [13–15]. Using orthogonal arrays significantly reduces the number of experimental configurations to be studied. Furthermore, the conclusions drawn from small scale experiments are valid over the entire experimental region spanned by the control fac-

* Corresponding author. Tel.: +86 0993 2055015; fax: +86 0993 2057270.
E-mail addresses: dengh@yahoo.com.cn, dengh216@sina.com (H. Deng).

0304-3894/$ – see front matter © 2010 Elsevier B.V. All rights reserved.
doi:10.1016/j.jhazmat.2010.06.018

Nomenclature

A	Temkin isotherm constant related to adsorption capacity (L/mg) (L/g)
AC	activated carbon
ANOVA	analysis of variance
b	the Langmuir constant
B	Temkin constant related to heat of sorption (J/mol)
C_0	the highest initial dye concentration (mg/L)
C_e	equilibrium concentration (mg/L)
D_p	average pore diameter (nm)
df	the degree of freedom
FT-IR	Fourier transform infrared spectroscopy
K_L	Langmuir isotherm constant related to adsorption capacity (L/mg)
K_F	Freundlich isotherm constant related to adsorption capacity (mg/g)
k_1	rate constant of pseudo-first-order (min^{-1})
k_2	pseudo-second-order rate constant (g/mg/min)
M	weight of activated carbon
M_0	weight of air-dried cotton stalk
MB	methylene blue
$1/n$	Freundlich isotherm constant related to adsorption intensity
OAD	orthogonal array design
PSD	pore size distribution
q_e	the amount of dye adsorbed (mg/g)
q_m	q_e for complete monolayer adsorption capacity (mg/g)
q_t	adsorption capacity at time t (mg/g)
R	gas constant (8.314 J/(mol K))
R_L	dimensionless separation factor
R^2	correlation coefficient
SEM	scanning electron microscopy
S_{BET}	BET surface area (m^2/g)
S_{ext}	external surface area (m^2/g)
S_{mic}	micropores surface area (m^2/g)
SS	the sum of the square
T	absolute temperature (K)
t	contact time (min)
V	the volume of solution (L)
V_t	total pore volume (cm^3/g)
V_{mic}	micropores pore volume (cm^3/g)

tors and their settings [16]. The objective of this study was to use the Taguchi method, one of the orthogonal array designs, to optimize the preparation conditions of AC from cotton stake. The effects of the preparation variables such as impregnation time, radiation power, radiation time and concentration of phosphoric acid on iodine number and carbon yield were investigated subsequently. Also, the Taguchi method was used to find the best level of each parameter in the preparation of AC. The characteristics and the adsorption ability of the AC prepared under optimized conditions were investigated, as well.

2. Experimental

2.1. Materials

Cotton stalk was provided from a local farm in Shihezi, Xinjiang Province in China. Phosphoric acid (98 wt.%) was supplied by Xi'an Chemicals & Reagent Corp of China. All other chemicals used in this study were analytical grade and purchased from Xi'an Chemicals & Reagent Corp of China.

Table 1
Design factors and levels.

Independent variable	Symbol	Range and levels			
		1	2	3	4
Radiation power (W)	A	320	400	480	560
Radiation time (min)	B	6	7	8	9
Concentration of H_3PO_4 (vol.%)	C	30	40	50	60
Impregnation time (h)	D	16	20	24	28

2.2. Preparation of AC

Cotton stalk was used as the raw material for the preparation of AC. Cotton stalk was washed several times with distilled water to remove impurities and then it was dried in oven at 80 °C until constant weight. After that, cotton stalk was milled and sieved into a uniform size of less than 2.0 mm. The chemical compositions of cotton stalk were given elsewhere [17].

Dried cotton stalk samples with the mass of 6 g were mixed with 30 mL of H_3PO_4 to vary concentrations in the range of 30–60% by volume. The slurry was kept at room temperature for various time spans in the range of 16–28 h to ensure the access of the H_3PO_4 to the cotton stalk. After mixing, the slurry was placed in a ML-3 type sequence MW heating apparatus which produced by Sichuan university (Sichuan Province, China). The experimental apparatus is same to that described elsewhere [17]. After a certain microwave heating power and microwave radiation time, the carbonized samples were washed sequentially with 0.05 M NaOH, hot water and cold distilled water until the pH of the washing solution reached 6–7, filtered and finally dried at 105 °C.

2.3. Optimization of AC preparation conditions

In order to optimize the preparation conditions of the AC, Taguchi experimental design method was used. An L_{16} orthogonal array with four operational parameters each in four levels was used to evaluate the corresponding optimal values. These variables and their levels are summarized in Table 1. The complete design matrix of the experiments and the obtained results are shown in Table 2. Iodine is considered as probe molecules for assessing the adsorption capacity of sorbents for solutes of molecular sizes less than 10 Å. Iodine number was normally listed as specification parameter for commercial ACs. Therefore, the responses were iodine number (Y_1, mg/g) and AC yield (Y_2, %). Iodine number (q_{iodine}, mg/g carbon) of AC was obtained at 20 ± 1 °C on the basis of the Standard

Table 2
Experimental design matrix and results.

Runs	Variables				Responses (Y)	
	A	B	C	D	Iodine number (Y_1, mg/g)	Yield of the AC (Y_2, %)
1	1	1	1	1	733.45	22.94
2	1	2	2	2	747.37	34.25
3	1	3	3	3	798.00	40.58
4	1	4	4	4	759.70	38.08
5	2	1	2	3	758.64	28.27
6	2	2	1	4	763.78	36.03
7	2	3	4	1	843.28	43.87
8	2	4	3	2	885.14	42.95
9	3	1	3	4	787.35	32.13
10	3	2	4	3	763.20	40.15
11	3	3	1	2	758.42	35.79
12	3	4	2	1	745.36	37.73
13	4	1	4	2	741.37	30.43
14	4	2	3	1	770.75	38.05
15	4	3	2	4	759.42	37.50
16	4	4	1	3	728.13	35.43

Table 3
Adsorption models adopted in this work and their parameters.

Isotherm	Equation	Parameters
Freundlich isotherm	$q_e = K_F C_e^{1/n}$	K_F (L/mg): the Freundlich adsorption constant n: the empirical parameter representing the energetic heterogeneity of the adsorption sites (dimensionless) q_e (mg/g): the amount of dye adsorbed
Langmuir isotherm	$q_e = \frac{q_m K_L C_e}{1+K_L C_e}$	C_e (mg/L): the equilibrium concentration q_m (mg/g): complete monolayer adsorption capacity K_L (L/mg): the equilibrium adsorption constant
Temkin isotherm	$q_e = \frac{RT}{B} \ln(K_T C_e)$	B (J/mol): the Temkin constant related to heat of sorption K_T (L/g): the Temkin isotherm constant R (8.314 J/(mol K)): the gas constant T (K): the absolute temperature
Pseudo-first-order	$\frac{dq_t}{dt} = k_1(q_e - q_t)$	q_e (mg/g): equilibrium adsorption capacity q_t (mg/g): adsorption capacity at time t t (min): contact time k_1 (min^{-1}): rate constant of pseudo-first-order
Pseudo-second-order	$\frac{dq_t}{dt} = k_2(q_e - q_t)^2$	q_t (mg/g): adsorption capacity at time t k_2 (g/mg/min): pseudo-second-order rate constant

Test Method, ASTM Designation D4607-86 [18]. The yield of the carbon samples was estimated according to

$$Y = \frac{M}{M_0} \times 100 \quad (1)$$

where M is the weight of AC and M_0 is the weight of air-dried cotton stalk. In order to investigate the influence of operational parameters on the adsorption ability and the yield of the prepared AC, the collected data was analyzed with the statistical analysis software, SPSS, version 13.0 (SPSS, Inc., Chicago, IL, USA).

2.4. Characterization of AC

The surface physical morphology of AC and cotton stalk were identified by using SEM technique. A JSM-6390LV (JEOL Ltd, Japan) with a 3 kV accelerating voltage was used to characterize the morphology of the sample which was dried overnight at approximately 105 °C under vacuum before SEM analysis. The surface area and the porosity of the AC prepared at optimized conditions were characterized by N_2 adsorption–desorption isotherms. ASAP2020 (Micromeritics Ltd., USA) was used to determine the surface areas and total pore volumes. The S_{BET} was calculated by the BET equation, micropore volume and micropore specific surface area were obtained using the t-plot method, and pore size distribution (PSD) was determined using the BJH model [19]. An FT-IR spectroscope (AVATAR 360, Thermo Nicolet Co., USA) with KBr pellet was used to study the surface functional groups of the AC. The zero surface charge characteristic of the AC was determined by using the solid addition method [20]. The ability of AC in the adsorption of MB was investigated by batch isotherm and kinetic studies.

2.5. Batch equilibrium

The 100-mL samples of MB solution with known concentration and the samples of the produced AC with the mass of 0.40 g were added to Erlenmeyer flasks. The flasks were shaken in a shaker incubator in an isothermal condition of 25 ± 1 °C and shaking speed of 160 rpm for 2 h to reach adsorption equilibrium conditions. Then the samples were filtered and the residual concentration of MB in the filtrate was analyzed by a double beam UV–vis spectrophotometer (Hitachi Co., Japan) at 665 nm. The amount of MB adsorbed per unit mass of adsorbent at equilibrium conditions, q_e (mg/g), was calculated by [21]:

$$q_e = \frac{(C_0 - C_e)}{M} \times V \quad (2)$$

where C_0 (mg/L) and C_e (mg/L) are the initial and the equilibrium concentrations of MB at solutions, respectively. V (L) is the volume of solution and M (g) is the mass of AC. We used different models, Langmuir, Freundlich and Temkin to investigate the equilibrium behavior of MB adsorption on the prepared AC samples. They are described in Table 3.

Another characteristic parameter of the Langmuir isotherm is the dimensionless factor R_L (separation factor), related to the shape of the isotherm. Its value indicates either unfavorable ($R_L > 1$), linear ($R_L = 1$), favorable ($0 < R_L < 1$) or irreversible ($R_L = 0$) adsorption and it is evaluated as [22]:

$$R_L = \frac{1}{b + C_0} \quad (3)$$

where b is the Langmuir constant and C_0 (mg/L) is the highest concentration of the adsorbate.

2.6. Batch kinetic

The kinetic experiments were performed using a procedure similar to the equilibrium studies. Samples containing 1500 mg/L pollutant with the volume of 100 mL were prepared in the Erlenmeyer flasks. Produced AC sample (0.40 g) was added to each flask. The flasks were shaken at 26 ± 1 °C and 160 rpm. At different time intervals the concentration of the residual pollutant in the solution was analyzed by the same procedure as batch equilibrium studies. The amount of pollutant adsorbed at each time interval per unit mass of the adsorbent, q_t (mg/g), was calculated by the following formula [21]:

$$q_e = \frac{(C_0 - c_t)}{M} \times V \quad (4)$$

where C_0 (mg/L) is initial liquid-phase concentration of the pollutant and C_t (mg/L) is its concentration at time t. V (L) is the volume of the solution and M (g) is the mass of the adsorbent. In order to determine the best kinetic model which fits the adsorption experimental data, the pseudo-first-order, pseudo-second-order were examined. They are described in Table 3.

Table 4
ANOVA of the activated carbon yield.

Source	*SS*	*df*	Mean square	*F*	*P*
A	31.559	3	10.520	7.291	0.068
B	306.430	3	102.143	70.790	0.003
C	98.999	3	33.000	22.870	0.014
D	0.437	3	0.146	0.101	0.954
Error	4.329	3	1.443		
Total	21046.921	16			

3. Results and discussion

3.1. Optimization of AC preparation

3.1.1. Main factors

According to the L_{16} array designed by Taguchi method, 16 different AC samples were prepared. Iodine number and yield of each sample were determined and shown in Table 2. The results of ANOVA analysis are shown in Tables 4 and 5. The ANOVA was done at 95% confidence level and established on the sum of the square (*SS*), the degree of freedom (*df*), the mean square, *F* value and *P* value. *P* value, last column in tables indicates whether the factor will affect the response of AC or not. A *P* value, which is lower than 0.05, means that this factor is important to the response. Table 4 describes that both radiation time and concentration of H_3PO_4 were significant factors for the yield of AC. However, the radiation time with the biggest *F* value of 70.790 was the most important factor affecting the carbon yield followed by the concentration of H_3PO_4, radiation power and impregnation time. Table 5 shows that not all factors were significant impact factors affected the iodine number of AC, because their *P* values were all greater than 0.05. Among these factors, the concentration of H_3PO_4 has the greatest effect on iodine number with the highest F value. The effects on iodine number are decreased gradually in radiation power, radiation time and impregnation time.

3.1.2. Effect of independent variable on AC preparation

Fig. 1 shows that both the yield and the adsorption ability of AC samples were increased, enhancing radiation power (parameter *A*) up to 400 W. One possible reason is that pore structure on the surface of AC was fully developed at the power up to 400 W. The yield and the adsorption ability of the AC reduced when radiation power increased up to 480 W. A small quantity of carbon was possibly burnt out and pore structure on its surface destroyed under overfull energy. Similar results have been obtained by other researchers [8,17].

As shown in Fig. 1, the adsorption ability of the AC increased gradually lengthening activation time (parameter *B*) up to 8 min while it decreased as excessive extension of activation time up to 9 min. There was similar tendency of carbon yield. It was also found by Li et al. when they prepared the AC from tobacco stems using microwave radiation [23]. The improvement of activation degree depended on the microwave radiation time. With the prolongation of microwave radiation time, more and more active sites and pores were formed on the surface of samples. Therefore, the adsorption capacity of AC would be increased along with the prolongation of microwave radiation time. However, the pores of carbon would be burnt off by microwave heating, when microwave radiation time reached a certain value, which would lower the iodine number and the yield of AC.

Table 5
ANOVA of iodine number.

Source	*SS*	*df*	Mean square	*F*	*P*
A	9470.583	3	3156.861	5.975	0.088
B	3078.552	3	1026.184	1.942	0.300
C	10167.308	3	3389.103	6.414	0.081
D	971.179	3	323.726	0.613	0.651
Error	1585.060	3	528.353		
Total	9547681.187	16			

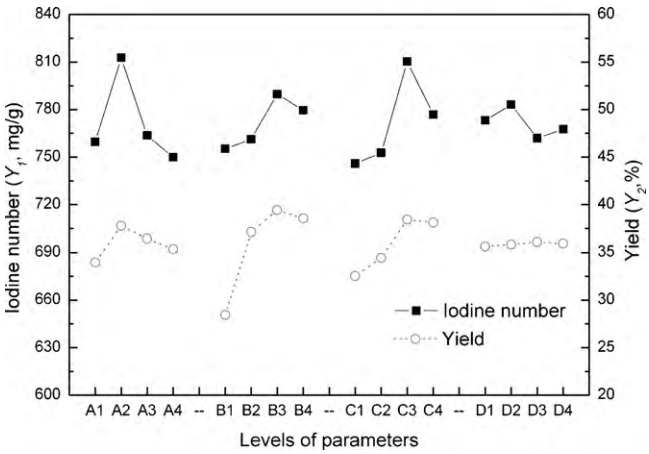

Fig. 1. The effect of operational parameters on responses of the prepared AC samples ((A) radiation power, (B) radiation time, (C) concentration of H_3PO_4, and (D) impregnation time).

Fig. 1 shows the results of ANOVA analysis for the effect of the concentration of phosphoric acid (parameter *C*) on the yield and the iodine numbers. Enhancing the concentration of H_3PO_4 from 30% to 50% by volume increased the yield and the iodine numbers of the prepared AC samples. This is perhaps due to an enhancement of the formation of micropores on the AC, which are much more effective in adsorption process and increase the adsorption ability of the adsorbents [24]. The yield and the iodine numbers of the prepared samples were decreased by exceeding the phosphoric acid concentration up to 60% by volume. The observed reduction in the sample due to the excess of H_3PO_4 content could be attributed to the possible formation of phosphates via interaction with the inorganics present under pyrolysis action, which may block some of the pores present [25]. These salts would be leached out by 0.05 M NaOH in the end. This assumption will be confirmed later by FT-IR spectra through the appearing phosphate band.

The results presented in Fig. 1 also shows that impregnation time (parameter *D*) had little influence on the yield, but it had a little effect on the adsorption ability. The action of H_3PO_4 on the lignocellulosic material could be expected as the following mechanism. During impregnation stage the acid attacked the cellular structure of cotton stalk, forming cleavage to the linkages between the lignin and cellulose. It was followed by recombination reactions, where larger structural units and strong cross linked solids were formed. This acid worked, principally, in early stage during impregnation and might be extended to have a slight effect in the carbonization stage [26].

3.1.3. Optimized conditions

In the production of commercial ACs, relatively high product yield and adsorption capacity were expected. Therefore, more attention should be paid to improve the carbon yield and enhance its adsorption capacity for economical viability. However, it was difficult to optimize both these responses under the same condition, for the different interest in different region. Therefore, in order to compromise the two responses, two experimental conditions with the highest desirability were selected to verify. The optimum conditions were radiation power of 400 W, radiation time of 8 min, concentration of H_3PO_4 of 50% by volume and impregnation time of 20 h.

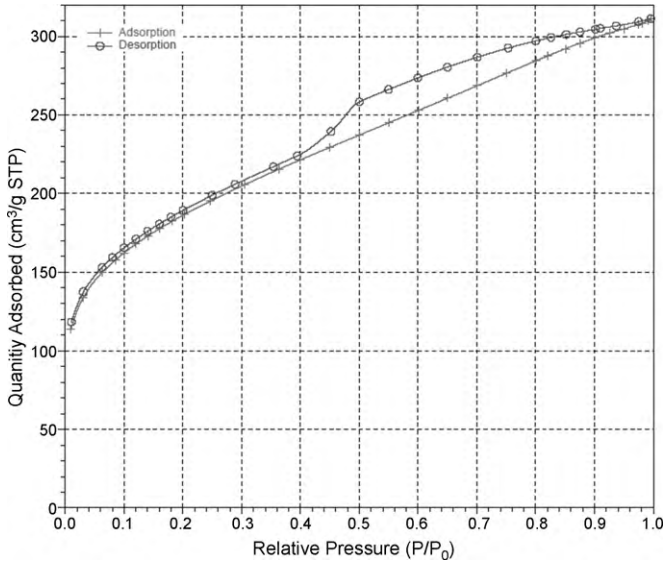

Fig. 2. Adsorption–desorption isotherms of N_2 at −196 °C on the AC prepared at optimized conditions.

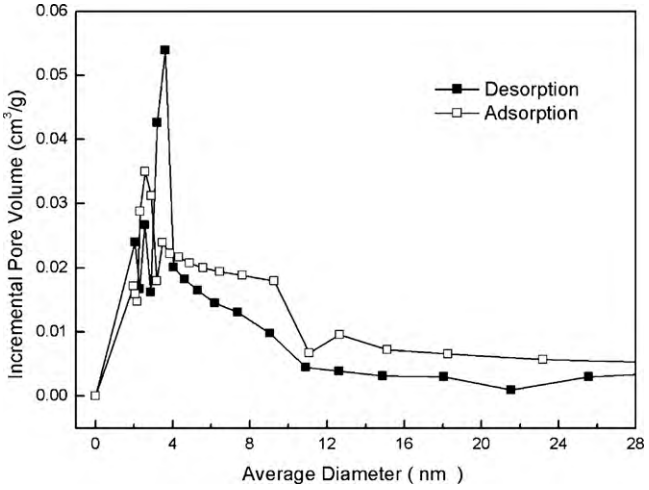

Fig. 3. Pore size distributions of the AC prepared at optimized conditions by BJH method.

3.2. Pore structure of the AC prepared under optimized condition

The structural heterogeneity of AC plays an important role in adsorption processes, and numerous methods have consequently been developed and applied for the characterization of this property. In this study, we used nitrogen adsorption and SEM methods to characterize our carbon sample prepared under optimum conditions.

3.2.1. Nitrogen adsorption

Nitrogen adsorption, because the relatively small molecule diameter of nitrogen is frequently used at −196 °C to probe porosity and surface area and to be a standard procedure for the characterization of porosity texture of carbonaceous adsorbents. The adsorption isotherm is the information source about the porous structure of the adsorbent, heat of adsorption, characteristic of physical and chemical and so on. Adsorption isotherm may be grouped six types. Fig. 2 illustrates adsorption–desorption isotherms of N_2 at −196 °C on AC. As illustrated in Fig. 2, AC exhibited adsorption isotherm of type IV according to IUPAC [27]. The type IV isotherm is characteristic properties of solids having both micro and mesopores. The initial part of the isotherm followed the same path as the corresponding type II isotherm and therefore the result of monolayer–multilayer adsorption on the mesopore walls [28].

The BET surface area (S_{BET}), external surface area (including only mesopores S_{ext}), micropores surface area (S_{mic}), total pore volume (V_t), micropores pore volume (V_{mic}) and average pore diameter (D_p) results obtained by applying the BET equation to N_2 adsorption at −196 °C are listed in Table 6.

Table 6
Porous structure parameters of the CSAC.

Typical parameters	
S_{BET} (m^2/g)	652.82
S_{ext} (m^2/g)	525.64
S_{mic} (m^2/g)	127.18
V_t (cm^3/g)	0.476
V_{mic} (cm^3/g)	0.0578
D_p (nm)	2.92

3.2.2. Characterization of pore structure

Pore size distribution (PSD), a very important property of adsorbents, determines the fraction of the total pore volume accessible to molecules of a given size and shape. According to the classification of IUPAC-pore dimensions, the pores of absorbents can be grouped into micropores (d < 2 nm), mesopore (d = 2–50 nm) and macropore (d > 50 nm). Fig. 3 shows the pore size distribution was calculated in the standard manner by using BJH method [29]. It appears that the AC included both micro and mesopores. Percentages of micropores and mesopores area were 19.5% and 80.5%, respectively. The different textural characteristics of the AC were found by Li et al. [30], Girgis et al. [31] and El-Hendawy et al. [5], their ACs included large number of micropores. Microwave heating generates heat within the material and heats the entire volume at about the same rate. This heating process could quicken the diffusing rate of the volatilizable matter inside the AC and fasten its releasing rate from the surface of AC, which makes more mesopores available possibly.

3.2.3. Surface morphology

SEM technique was employed to observe the surface physical morphology of the AC. Fig. 4 shows the SEM micrograph of the cotton stalk before and after the carbonization at the optimum preparation conditions. For the raw cotton stalk (Fig. 4a), the surface was relatively organized without any pores except for some occasional cracks. The SEM images of the AC (Fig. 4b and c) show that the external surfaces were full of cavities and quite irregular as a result of activation. Fig. 4d appears that there were many macropores of width more than 0.2 mm that might be ink-bottle shaped on the surface of this carbon, indicating the aggressive attack of the reagent with the cotton stalk during impregnation. Those pores resulted from the evaporation of the chemical reagent (H_3PO_4) during carbonization, leaving the space previously occupied by the reagents.

3.3. Surface chemical structure of the AC prepared under optimized condition

3.3.1. Zero surface charges

The pH_{ZPC} of an adsorbent is a very important characteristic that determines the pH at which the adsorbent surface has net electrical neutrality. Fig. 5 shows the plot between ΔpH, i.e. (pH_0–pH_f) and pH_0 for pH_{ZPC} measurement. The point of zero charge for the AC was found to be 6.00. It was lower than that of AC prepared from cotton stalk with $ZnCl_2$ as activation under microwave radiation [17]. But it was higher than that of AC prepared from cotton stalk with KH_2PO_4

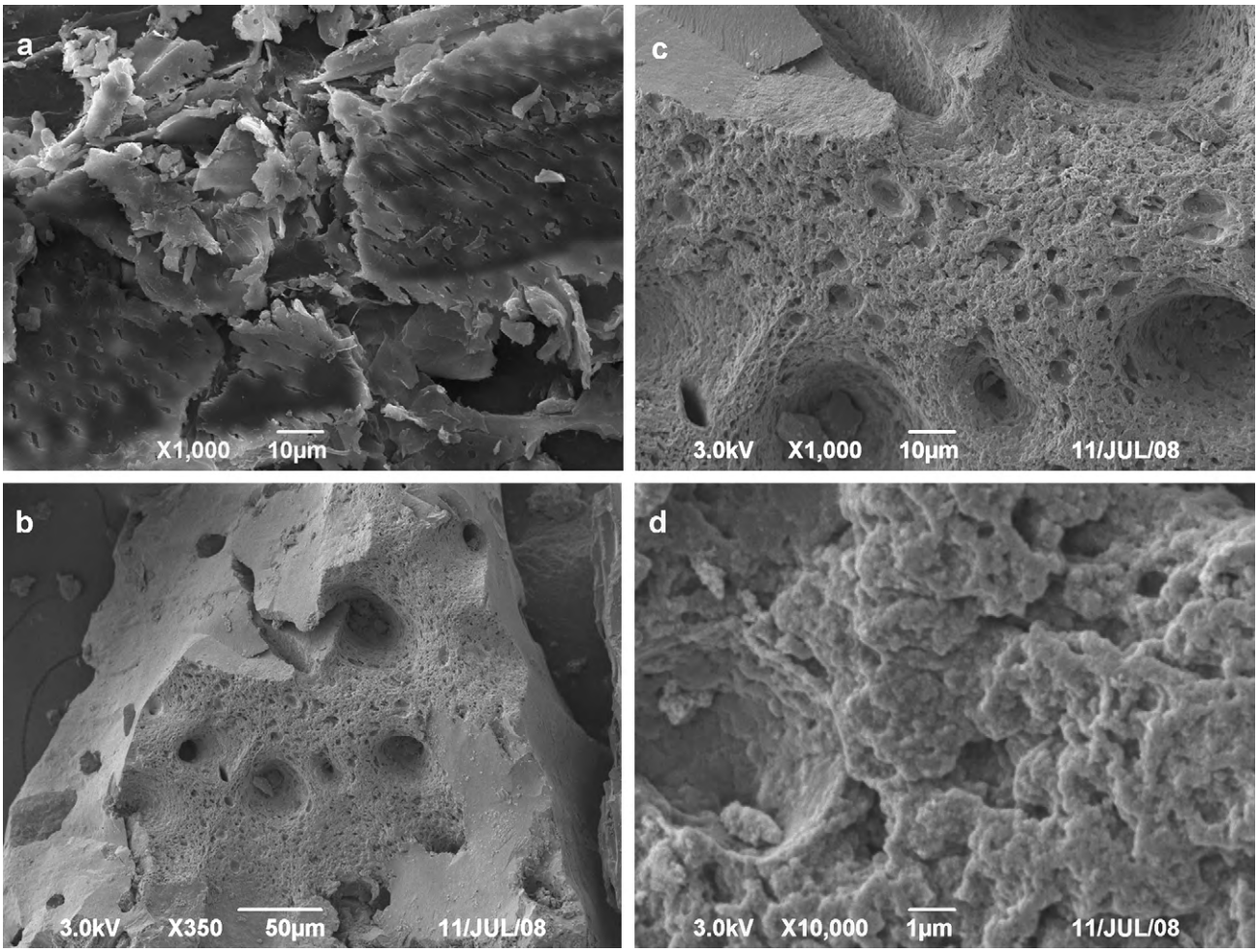

Fig. 4. SEM micrographs of the cotton stalk (a) and the AC prepared at optimized conditions (b, c and d).

as activation [30]. And it was also higher than that of AC prepared from jackfruit peel waste by H_3PO_4 chemical activation [32]. These results indicated that the pH_{ZPC} of AC was depended on the raw material and the activated agency.

3.3.2. Functional groups

Three main components of cotton stalk are cellulose, hemicellulose and lignin. The expected oxygen function groups in cotton stalk

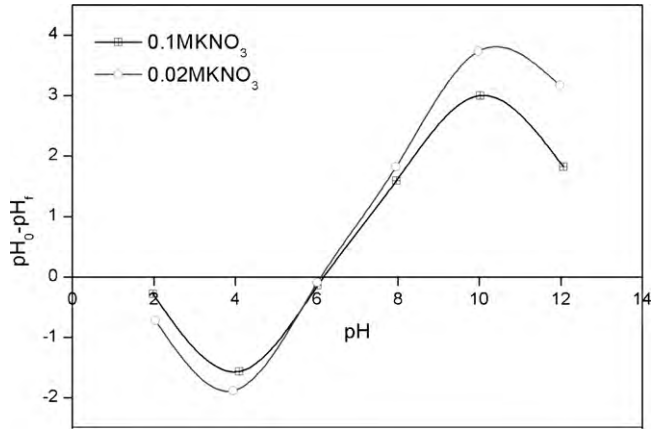

Fig. 5. Determination of the point of zero charge of the AC prepared at optimized conditions by the solid addition method.

are hydroxyl, ether, carbonyl acetoxy, etc. According research from El-Hendawy et al. [26], cotton stalk displayed the following bands: the band at 3495 cm^{-1} was attributed to O–H stretching in hydroxyl functional groups, the band at 2950 and 2880 cm^{-1} were ascribed to ν C–H and δ C–H (ν = stretching and δ = bending) absorption bands that may be present in methyl and methylene groups, the band at 1745 cm^{-1} was ascribed to C=O stretching from ketones, aldehydes or carboxylic groups, the band at 1260 cm^{-1} was attributed to C–O–C stretching in ethers and the later band at 817 cm^{-1} was attributed to out-of-plane bending in benzene derivatives.

To characterize surface groups on the AC, FT-IR spectra were obtained. FT-IR spectra of the AC are shown in Fig. 6. It was seen that the absorbance bands have several peaks at 1627.7, 1584.2, 1362.2, 1342.6 and 966.3 cm^{-1}. Most of these bands have been reported by other investigators for different carbon materials. The peak at 1627.7 and 1584.2 cm^{-1} were the characteristics of the C=O stretching vibration of laconic and carbonyl groups [33,34]. The peaks occurring at 1362.2 and 1342.6 cm^{-1} were all ascribed to oxygen functionalities such as highly conjugated C–O stretching, C–O stretching in carboxylic groups and carboxylate moieties [35,36]. The band at around 966.3 cm^{-1} was characteristic to P=O groupsand to P=O stretching in linear and cyclic polyphosphate and inorganic species [30].

Significant changes in the spectra of the AC were observed which, in particular, concern the bands located in the two regions. In the region from 3500 to 2800 cm^{-1} where two bands disappeared and at 966 cm^{-1} where one new band appeared. These results suggested that under carbonization and activation process many weak

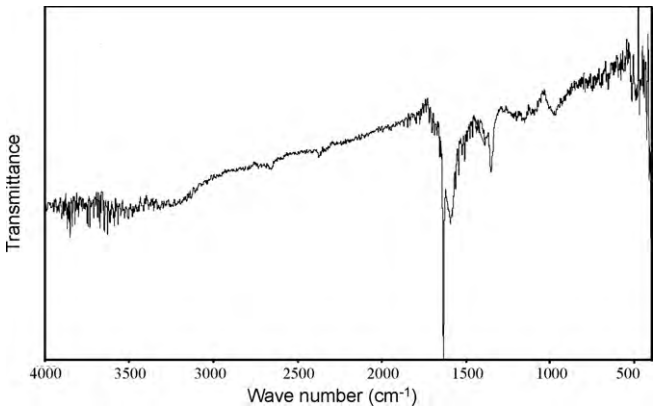

Fig. 6. Fourier transform infrared spectra of the AC prepared at optimized conditions.

bonds disappeared, at the same time, polyphosphate and inorganic species were formed in the carbon.

3.4. MB adsorption on the AC prepared under optimized conditions

3.4.1. Equilibrium adsorption isotherms

The Langmuir, Freundlich and Temkin models were fitted the experimental data and the results are shown in Table 7. The values of correlation coefficients showed that the experimental data of MB adsorption were fitted the Langmuir isotherm better than the others ($R = 0.9800$). This implied the homogeneous and the monolayer coverage of MB on the AC surface. The maximum MB adsorption capacity on the AC (q_m) was 245.70 mg/g and the dimensionless separation factor for MB adsorption was calculated equal to 0.0322 which showed the MB adsorption was favorable. According to the $1/n$ value (0. 1609) calculated from Freundlich isotherm, the adsorption of MB on the AC was favorable. Since the correlation coefficients resulted from fitting the experimental data to Temkin isotherms was less than 0.9, it was not used to analyze the adsorption process of MB on the AC surface. The similar phenomenon has also been observed by Hameed et al. [37].

3.4.2. Kinetics of adsorption

The experimental data of MB adsorption on the AC in different time intervals were examined to fit pseudo-first-order and pseudo-second-order models, using the plots of $\log(q_e - q_t)$ against t and t/q_t versus t, respectively. The corresponding results are shown in Table 8. The correlation coefficients resulted from the second-order model were higher than the first-order model for the adsorption of MB. Therefore, the pseudo-second-order model could better describe the kinetics of the adsorption of the MB on the AC.

Table 7
Isotherm parameters for MB adsorption onto AC ($T = 26\,^{\circ}C$, $m = 0.4$ g and $V = 100$ mL, pH = 7, agitation rate = 160 rpm and $t = 2$ h).

Isotherms	Parameters	
Langmuir	q_m (mg/g)	245.70
	K_L (L/mg)	1.55×10^{-2}
	R_L	3.22×10^{-2}
	R	0.9800
Freundlich	K_F (L/mg)	75.00
	$1/n$	0.1609
	R	0.9089
Temkin	K_T (L/mg)	42.80
	B (J/mol)	115.50
	R	0.8678

Table 8
Parameters of the kinetic models for MB adsorption onto AC ($T = 26\,^{\circ}C$, $m = 0.4$ g and $V = 100$ mL, pH = 7, agitation rate = 160 rpm and $C_0 = 1500$ mg/L).

models	Parameters	
Pseudo-first-order model	k_1 (min^{-1})	0.0389
	$q_{e,cal}$ (mg/g)	264.24
	R^2	0.8848
Pseudo-second-order model	k_2 (g/mg/min)	1.72×10^{-4}
	$q_{e,cal}$ (mg/g)	244.50
	R^2	0.9818

4. Conclusions

Taguchi method was used to optimize the preparation of AC from cotton stalk with H_3PO_4 as activator. Radiation time and concentration of H_3PO_4 were significant factors for the AC yield. Concentration of phosphoric acid was the greatest impact factor on iodine number of the AC. The optimum conditions were radiation power of 400 W, radiation time of 8 min, concentration of H_3PO_4 of 50% by volume and the impregnation time of 20 h. N_2 adsorption showed BET surface area of prepared AC was 652.82 m^2/g, where the carbon included both micro and mesopores. Percentage of micropore and mesopore area is determined as 19.5% and 80.5%, respectively. Scanning electron microscopy (SEM) and Fourier transform infrared spectroscopy (FT-IR) investigations evidenced that the presence of opened-pore structure and different functionalities on the carbon surfaces compared with those of cotton stalk. Langmuir isotherm better fits the experimental equilibrium data of MB adsorption on the prepared AC. The maximum MB adsorption capacity on the AC is 245.70 mg/g. The adsorption of MB fits the pseudo-second-order kinetic model.

References

[1] R.C. Bansal, J.-B. Donnet, F. Stoeckli, Active Carbon, Marcel Dekker, Inc., New York, 1988.
[2] C.P. Huang, in: P.N. Cheremis in off, F. Ellerbusch (Eds.), Carbon Adsorption Handbook, second ed., J. Ann. Arbor Sci. Pub., Inc., Michigan, 1980.
[3] A. Bota, K. Laszlo, L. Nagy, G. Lajos, T. Copitzky, Comparative study of active carbons from different precursors, J. Langmuir 13 (1997) 6502–6509.
[4] B.S. Girgis, M.F. Ishak, Activated carbon from cotton stalks by impregnation with phosphoric acid, J. Mater. Lett. 39 (1999) 107–114.
[5] A.A. El-Hendawy, A.J. Alexander, R.J. Andrews, G. Forrest, Effects of activation schemes on porous, surface and thermal properties of activated carbons prepared from cotton stalks, J. Anal. Appl. Pyrol. 82 (2008) 272–278.
[6] A.A.M. Daifullah, B.S. Girgis, Impact of surface characteristics of activated carbon on adsorption of BTEX, J. Colloids Surf., A: Physicochem. Eng. Asp. 214 (2003) 181–193.
[7] L.M. Norman, C.Y. Cha, Production of activated carbon from coal chars using microwave energy, J. Chem. Eng. Commun. 140 (1996) 87–110.
[8] L. Wei, Zh. Libo, P. Jinhui, L. Ning, Zh. Xueyun, Preparation of high surface area activated carbons from tobacco stems with K_2CO_3 activation using microwave radiation, J. Ind. Crops Prod. 27 (2008) 341–347.
[9] J. Yongbin, L. Tiehu, Zh. Li, W. Xiaoxian, Q. Lin, Preparation of activated carbons by microwave heating KOH activation, J. Appl. Surf. Sci. 254 (2007) 506–512.
[10] G. Taguchi, System of Experimental Design, Krus International, New York, 1986.
[11] R.K. Roy, A Primer on Taguchi Method, Van Nostrand Reinhold, New York, 1990.
[12] Zh. Guanghua, J. Huangxian, Determination of naproxen with solid substrate room temperature phosphorimetry based on an orthogonal array design, J. Anal. Chim. Acta 506 (2004) 177–181.
[13] Y. Yadollah, S. Abolfazl, K. Mostafa, Orthogonal array design for the optimization of supercritical carbon dioxide extraction of platinum(IV) and rhenium(VII) from a solid matrix using cyanex 301, J. Sep. Purif. Technol. 61 (2008) 109–114.
[14] M. Yueyu, H. Henry, N. Derek, N. Xueyuan, Optimization of the electrolytic plasma oxidation processes for corrosion protection of magnesium alloy AM50 using the Taguchi method, J. Mater. Process. Technol. 182 (2007) 58–64.
[15] S. Aber, A. Khataee, M. Sheydaei, Optimization of activated carbon fiber preparation from Kenaf using K_2HPO_4 as chemical activator for adsorption of phenolic compounds, Bioresour. Technol. 100 (2009) 6586–6591.
[16] S.M. Phadke, Quality Engineering Using Robust Design, Prentice Hall, New Jersey, 1989.
[17] H. Deng, L. Yang, G.H. Tao, J.L. Dai, Preparation and characterization of activated carbon from cotton stalk by microwave assisted chemical activation—application in methylene blue adsorption from aqueous solution, J. Hazard. Mater. 166 (2009) 1514–1521.

[18] R.-S. Juang, F.-C. Wu, R.-L. Tseng, Mechanism of adsorption of dyes and phenols from water using activated carbons prepared from plum kernels, J. Colloid Interface Sci. 227 (2000) 437–444.
[19] S.J. Gregg, K.S. Sing, Adsorption, Surface Area and Porosity, Academic Press, London, 1982.
[20] A. Kumar, B. Prasad, I.M. Mishra, Adsorptive removal of acrylonitrile by commercial grade activated carbon: kinetics, equilibrium and thermodynamics, J. Hazard. Mater. 152 (2008) 589–600.
[21] N. Daneshvar, D. Salari, S. Aber, Chromium adsorption and Cr(VI) reduction to trivalent chromium in aqueous solutions by soya cake, J. Hazard. Mater. 94 (2002) 49–61.
[22] K.R. Hall, L.C. Eagleton, A. Acrivos, T. Vermeulen, Pore- and solid-diffusion kinetics infixed-bed adsorption under constant-pattern conditions, J. Ind. Eng. Chem. Fundam. 5 (1966) 212–223.
[23] W. Li, Zh. Li-bo, P. Jin-hui, L. Ning, Zh. Xue-yun, Preparation of high surface area activated carbons from tobacco stems with K_2CO_3 activation using microwave radiation, J. Ind. Crops Prod. 27 (2008) 341–347.
[24] J.W. Kim, M.H. Sohn, D.S. Kim, S.M. Sohn, Y.S. Kwon, Production of granular activated carbon from waste walnut shell and its adsorption characteristics for Cu^{2+} ion, J. Hazard. Mater. 85 (2001) 301–315.
[25] M. Jagtoyen, F. Derbyshire, Activated carbons from yellow poplar and white oak by H_3PO_4 activation, Carbon 36 (1998) 1085–1097.
[26] A.-N.A. El-Hendawy, A.J. Alexander, R.J. Andrews, G. Forrest, Effects of activation schemes on porous, surface and thermal properties of activated carbons prepared from cotton stalks, J. Anal. Appl. Pyrol. 82 (2008) 272–278.
[27] K.W. Sing, D.H. Everet, R.A.W. Haul, L. Moscou, R.A. Pierotti, J. Rouquero, T. Siemieniewasa, Reporting physisorption data for gas/solid systems with special reference to the determination of surface area and porosity, J. Pure Appl. Chem. 57 (1985) 603–619.
[28] Z. Ryu, J. Zheng, M. Wang, B. Zhang, Characterization of pore size distributions on carbonaceous adsorbents by DFT, Carbon 37 (1999) 1257–1264.
[29] P.E.P. Barrett, L.G. Joyner, P.P. Halenda, Determination of pore volume and area distribution in porous substances. I. Computation of N_2 isotherms, J. Am. Chem. Soc. 73 (1951) 373–379.
[30] K. Li, Z. Zheng, X. Huang, G. Zhao, J. Feng, J. Zhang, Equilibrium, kinetic, thermodynamic studies on the adsorption of 2-nitroaniline onto activated carbon prepared from cotton stalk fibre, J. Hazard. Mater. 166 (2009) 213–220.
[31] B.S. Girgis, E. Smith, M.M. Louis, A.-N.A. El-Hendawy, Pilot production of activated carbon from cotton stalks using H_3PO_4, J. Anal. Appl. Pyrol. 86 (2009) 180–184.
[32] D. Prahas, Y. Kartika, N. Indraswati, S. Ismadji, Activated carbon from jackfruit peel waste by H_3PO_4 chemical activation: pore structure and surface chemistry characterization, Chem. Eng. J. 140 (2008) 32–42.
[33] C. Moreno-Castilla, M.V. López-Ramón, F. Carrasco-Marín, Changes in surface chemistry of activated carbons by wet oxidation, Carbon J. 38 (2000) 1995–2001.
[34] A. Abdel-Nasser, El-Hendawy, Influence of HNO_3 oxidation on the structure and adsorptive properties of corncob-based activated carbon, J. Carbon 41 (2003) 713–722.
[35] V. Boonamnuayvitaya, S. Sae-ung, W. Tanthapanichakoonc, Preparation of activated carbons from coffee residue for the adsorption of formaldehyde, Sep. Purif. Technol. 42 (2005) 159–168.
[36] C. Moreno-Castilla, F. Carrasco-Marín, A. Mueden, The creation of acid carbon surfaces by treatment with $(NH_4)_2S_2O_8$, J. Carbon 35 (1997) 1619–1626.
[37] B.H. Hameed, I.A.W. Tana, A.L. Ahmad, Optimization of basic dye removal by oil palm fibre-based activated carbon using response surface methodology, J. Hazard. Mater. 158 (2008) 324–332.